Proton Conduction in $La_{0.9}Sr_{0.1}Ga_{0.8}Mg_{0.2}O_{3-\alpha}$

Guilin Ma,*,† Feng Zhang,† Jianli Zhu,† and Guangyao Meng‡

Key Laboratory of Organic Synthesis of Jiangsu Province, School of Chemistry and Chemical Engineering, Suzhou University, Suzhou 215123, China, and Laboratory for Solid State and Chemistry and Inorganic Membrane, University of Science and Technology of China, Hefei 230026, China

Received June 2, 2006. Revised Manuscript Received October 16, 2006

The conduction behavior of $La_{0.9}Sr_{0.1}Ga_{0.8}Mg_{0.2}O_{3-\alpha}$ ceramics was investigated using electrochemical methods under various atmospheres in the temperature range of 600−1000 °C. The proton conduction in $La_{0.9}Sr_{0.1}Ga_{0.8}Mg_{0.2}O_{3-\alpha}$ ceramics is the first time it has been discovered in a hydrogen-containing atmosphere. The hydrogen concentration cell using $La_{0.9}Sr_{0.1}Ga_{0.8}Mg_{0.2}O_{3-\alpha}$ as an electrolyte showed stable electromotive forces close to the theoretical ones calculated from Nernst's equation, indicating the ion nature of the conduction. An isotope effect on the conductivity was observed using D_2O-Ar instead of H_2O-Ar as the atmosphere. The proton conduction in the specimen was directly confirmed by an electrochemical hydrogen permeation (hydrogen pumping) experiment. In a hydrogen atmosphere, $La_{0.9}Sr_{0.1}Ga_{0.8}Mg_{0.2}O_{3-\alpha}$ was found to be an excellent proton conductor, with a proton conductivity of $\sigma_H{}^+ = 1.4 \times 10^{-2}$ to 1.4×10^{-1} S cm^{-1} and a proton transport number of $t_H{}^+ > 0.99$, which are comparable to those of proton-conducting $BaCeO_3$-based oxides and $Ba_3Ca_{1.18}Nb_{1.82}O_{9-\alpha}$. In a water-vapor-containing air atmosphere, the specimen was found to be a mixed-ion (proton + oxide ion) conductor, and the proton and oxide-ion transport numbers were about 0.05−0.20 and 0.95−0.80, respectively, whereas in dry oxygen-containing atmospheres, the specimen was a pure oxide-ion conductor.

Introduction

It is well-known that high-temperature proton conductors are very important functional materials for their potential applications in some electrochemical devices and membrane reactors such as hydrogen fuel cell, hydrogen sensor, steam electrolyzer, separation and purification of hydrogen, hydrogenation and dehydrogenation of some organic compounds, and ammonia synthesis at atmospheric pressure, etc.[1−3]

Since the discovery of high-temperature proton conduction in doped perovskite-type $SrCeO_3$,[4] a number of materials such as doped $BaCeO_3$,[5] $AZrO_3$ (A = Ca, Sr, and Ba),[6,7] $KTaO_3$,[8,9] $Ln_2Zr_2O_7$,[10] Sr_2TiO_4,[11] $Ba_2SnYO_{5.5}$,[12] $LnScO_3$ (Ln = La, Nd, Sm, Gd),[13] and nonstoichiometric mixed perovskite-type $Ba_3Ca_{1+x}Nb_{2-x}O_9$[14−16] have been found to exhibit appreciable proton conduction under a hydrogen-containing atmosphere at elevated temperatures. The factors affecting proton conduction behavior of the materials were also investigated. In our previous researches, we determined and compared the proton conductivities and proton transport numbers of $BaCe_{0.9}Y_{0.1}O_{3-\alpha}$ and $BaCeO_3$.[17,18] $BaCe_{0.9}Y_{0.1}O_{3-\alpha}$ exhibited much higher ion conductivity σ_i and ion transport number t_i (e.g., $\sigma_i = 5.1 \times 10^{-2}$ S cm^{-1} and $t_i = 0.98$ at 1000 °C) than those of $BaCeO_3$ (e.g., $\sigma_i = 2.5 \times 10^{-4}$ S cm^{-1} and $t_i < 0.1$ at 1000 °C) in a hydrogen atmosphere, indicating that the existence of some oxygen vacancies in a sample is absolutely necessary. Also, we investigated[19] the relation between proton and/or oxide-ion conductivities and crystallographic free volume as well as tolerance factor t of $Ba_{1-x}La_xCe_{0.90-x}Y_{0.10+x}O_{3-\alpha}$ ($0 \le x \le 0.40$) and discovered that the proton and/or oxide-ion conductivities increase with the increasing free volume and tolerance factor. The tolerance factor ($t = 0.94$) of perovskite-type $BaCeO_3$ is higher than that ($t = 0.88$) of $SrCeO_3$, coinciding with the changing tendency of doped $BaCeO_3$ to usually have a higher proton and/or oxide-ion conductivities than doped $SrCeO_3$. According to the above observations, it may be expected that more

* Corresponding author. E-mail: 32uumagl@suda.edu.cn.
† Suzhou University.
‡ University of Science and Technology of China.

(1) Iwahara, H.; Asakura, Y.; Katahira, K.; Masahiro, T. *Solid State Ionics* **2004**, *168*, 299.
(2) Iwahara, H.; Shimura, T.; Matsumoto, H. *Electrochemistry* **2000**, *68*, 154.
(3) Marnellos, G.; Stoukides, M. *Science* **1998**, *282*, 98.
(4) Iwahara, H.; Esaka, T.; Uchida, H.; Maeda, N. *Solid State Ionics* **1981**, *3/4*, 359.
(5) Iwahara, H.; Uchida, H.; Ono, K.; Ogaki, K. *J. Electrochem. Soc.* **1988**, *135*, 529.
(6) Yajima, T.; Kazeoka, H.; Yogo, T.; Iwahara, H. *Solid State Ionics* **1991**, *47*, 271.
(7) Iwahara, H.; Yajima, T.; Hibino, T.; Ozaki, K.; Suzuki, H. *Solid State Ionics* **1993**, *61*, 65.
(8) Lee, W. K.; Nowick, A. S.; Boatner, L. A. *Solid State Ionics* **1986**, *18/19*, 989.
(9) Scherban, T.; Nowick, A. S.; Boatner, L. A.; Abraham, M. M. *Appl. Phys. A* **1992**, *55*, 324.
(10) Shimura, T.; Komori, M.; Iwahara, H. *Solid State Ionics* **1996**, 86−88, 685.
(11) Shimura, T.; Suzuki, K., Iwahara, H. *Solid State Ionics* **1998**, 113−115, 355.
(12) Murugaraj, P.; Kreuer, K. D.; He, T.; Schober, T.; Maier, J. *Solid State Ionics* **1997**, *97*, 1.
(13) Fujii, H.; Katayama, Y.; Shimura, T.; Iwahara, H. *J. Electroceram.* **1998**, *2* (2), 119.
(14) Liang, K. C.; Nowick, A. S. *Solid State Ionics* **1993**, *61*, 77.
(15) Liang, K. C.; Du, Y.; Nowick, A. S. *Solid State Ionics* **1994**, *69*, 117.
(16) Nowick, A. S.; Du, Y. *Solid State Ionics* **1995**, *77*, 137.
(17) Ma, G.; Shimura, T.; Iwahara, H. *Solid State Ionics* **1998**, *110*, 103.
(18) Ma, G.; Matsumoto, H.; Iwahara, H. *Solid State Ionics* **1999**, *122*, 237.
(19) Ma, G.; Shimura, T.; Iwahara, H. *Solid State Ionics* **1999**, *120*, 51.

10.1021/cm0612954 CCC: $33.50
Published on Web 11/16/2006

excellent proton conductors may be present in some perovskite-type oxides, which have a number of oxygen vacancies and larger tolerance factors. $LaGaO_3$ has a larger tolerance factor t ($t = 0.97$) than that of $SrCeO_3$ and $BaCeO_3$. Therefore, there may be a possibility of existing excellent proton conduction in $LaGaO_3$-based perovskite-type oxides.

Ishihara reported in 1994[20] that $LaGaO_3$ doped with Sr and Mg, $La_{0.9}Sr_{0.1}Ga_{0.8}Mg_{0.2}O_{3-\alpha}$, exhibits higher oxide-on conductivity than ZrO_2-based oxides, as well as pure oxide-ion conduction over a wide range of oxygen partial pressures from 1 to 1×10^{-20} atm. Hence $La_{0.9}Sr_{0.1}Ga_{0.8}Mg_{0.2}O_{3-\alpha}$ is regarded as a promising candidate electrolyte for an intermediate temperature fuel cell.[21] At the same time, Goodenough also reported that the cubic perovskite $La_{0.9}Sr_{0.1}Ga_{0.8}Mg_{0.2}O_{3-\alpha}$ has oxide-ion conductivity $\sigma_0 > 1 \times 10^{-2}$ S cm^{-1} at 600 °C with an oxide-ion transport number $t_O{}^{2-} \approx 1$ over the oxygen partial pressure range of 0.4 to 1×10^{-20} atm and that the conductivities of this oxide are the same in dry air, ambient air, and water-saturated (at room temperature) air, so there is no evidence of proton conduction in $La_{0.9}Sr_{0.1}Ga_{0.8}Mg_{0.2}O_{3-\alpha}$.[22] Fujii discovered the proton conduction in perovskite-type oxide ceramics based on $LnScO_3$ (Ln = La, Nd, Sm, or Gd) at high temperature.[13] At the same time, Lybye investigated the proton and oxide-ion conductivity of $La_{0.9}Sr_{0.1}Sc_{0.9}Mg_{0.1}O_{3-\alpha}$. According to the rules formulated by earlier researchers, doped $LaScO_3$ should be a better oxide-ion conductor than the gallate, but it was found that it is a proton conductor.[23]

To the best of our knowledge, until now there has been no report on the proton conduction in $La_{0.9}Sr_{0.1}Ga_{0.8}Mg_{0.2}O_{3-\alpha}$ except the work of Goodenough, but there is no evidence of proton conduction in his research mentioned above.[22] In the present work, we investigated electrochemically the proton conduction in $La_{0.9}Sr_{0.1}Ga_{0.8}Mg_{0.2}O_{3-\alpha}$ and found that it has a promising proton conduction, which is different from the earlier reported results.

Experimental Section

A ceramic specimen of $La_{0.9}Sr_{0.1}Ga_{0.8}Mg_{0.2}O_{3-\alpha}$ was synthesized by a solid-state reaction method. The required amounts of La_2O_3 (99.0%), $SrCO_3$ (99.0%), Ga_2O_3 (99.5%), and MgO (99.0%) reagents were fully mixed for 1 h in an agate mortar with ethanol, dried, and then calcined at 1300 °C for 8 h in air. The obtained oxides were ground with anhydrous ethanol using a planetary ball mill machine in an agate mill container and agate balls at 150 rpm for 5 h; they were then dried by infrared lamp, followed by sieving (100 mesh). The powder was pressed into pellets by a hydrostatic pressure of 2.5×10^3 atm and sintered at 1430 °C in air for 10 h. A dense ceramic pellet with a relative density of 96.5% was obtained. The phase structure of the ceramic specimen was determined by powder X-ray diffraction analysis with Cu Kα radiation (Rigaku D/MAX-IIIC X-ray diffractometer). The electrochemical measurements were conducted using the ceramic pellet (diameter 13 mm, thickness 1 mm) as electrolyte and porous platinum as electrode material in the temperature range of 600−1000 °C.

(20) Ishihara, T.; Matsuda, H.; Takita, Y. *J. Am. Chem. Soc.* **1994**, *116*, 3801.
(21) Feng, M.; Goodenough, J. B.; Huang, K.; Milliken, C. *J. Power Sources* **1996**, *63*, 47.
(22) Feng, M.; Goodenough, J. B. *Eur. J. Solid State Inorg. Chem.* **1994**, *31*, 663.
(23) Lybye, D.; Bonanos, N. *Solid State Ionics* **1999**, *125*, 339.

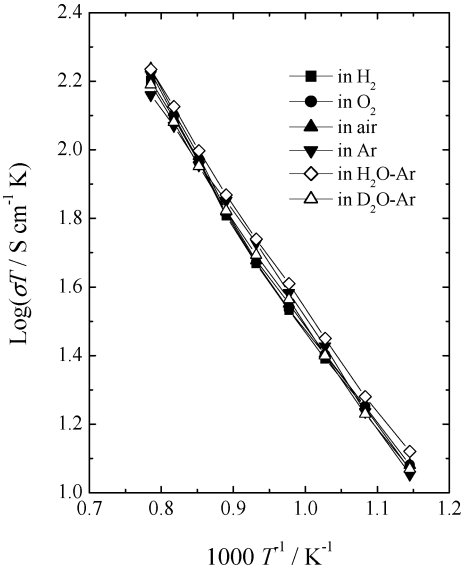

Figure 1. Dependence of the bulk conductivity of the specimen on temperature in various atmospheres.

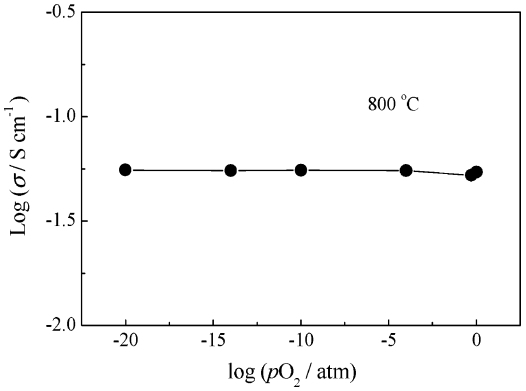

Figure 2. Dependence of the conductivity on oxygen partial pressure at 800 °C.

To estimate the contribution of proton and oxide ion to the conduction, the electromotive forces (EMFs) of the following gas concentration cells, including hydrogen, steam, and oxygen concentration cells, were measured

$$\text{Gas (I), Pt} \mid La_{0.9}Sr_{0.1}Ga_{0.8}Mg_{0.2}O_{3-\alpha} \mid \text{Pt, Gas (II)}$$

For the hydrogen concentration cell, the partial pressure of hydrogen gas, pH_2, was controlled by mixing hydrogen and argon using a gas blender. For the steam concentration cell, the partial pressure of water vapor, pH_2O, was controlled by saturating water vapor at a given temperature.

The conductivity of ceramic specimen was measured by the AC impedance method over the frequency range 1 Hz to 3 MHz using electrochemical workstations (Zahner IM6EX). The bulk conductivities as shown in Figures 1 and 2 were obtained from the bulk arc in the impedance spectra.

To verify the proton conduction in the ceramic specimen directly, we examined the electrochemical hydrogen permeation (hydrogen pumping) through the specimen by sending a direct current to the electrolytic cell

$$(+)\ H_2, \text{Pt} \mid La_{0.9}Sr_{0.1}Ga_{0.8}Mg_{0.2}O_{3-\alpha} \mid \text{Pt, Ar}\ (-)$$

Pure hydrogen at 1 atm was supplied to the anode chamber and dry argon was passed through the cathode chamber to carry the generated gas at the cathode to a hydrogen detector (Shanghai

Gainforce SG33A), where the concentration of the generated hydrogen gas was detected and the hydrogen evolution rate v in the standard state was calculated by using the following equation

$$v = \frac{273.15 V_{Ar} x}{(273.15 + T)S}$$

where V_{Ar} is the flow rate of the carrier gas (Ar), x is the concentration of the hydrogen gas generated in a mixed gas of hydrogen and argon, T is the surrounding temperature, and S is the area of the cathode. The theoretical rate was obtained on the basis of Faraday's law, assuming that the charge carriers in the specimen are only protons.

Results and Discussion

Conductivities under Various Atmospheres. Figure 1 shows the Arrhenius plots of the bulk conductivities of the specimen in hydrogen, oxygen, air, argon, H_2O-Ar (argon saturated with water vapor at 40 °C), and D_2O-Ar (argon saturated with deuterium-oxide vapor at 40 °C) atmospheres. Log(σT) increases basically in linearity on the reciprocal of the temperature, but there is slight difference in the conductivities at the same temperature under the different atmospheres. The values of the conductivity were around 1.4×10^{-2} to 1.4×10^{-1} S cm^{-1}, with activation energies of 59.3−61.2 kJ mol^{-1} in the temperature range of 600−1000 °C.

The dependence of the conductivity of $La_{0.9}Sr_{0.1}Ga_{0.8}Mg_{0.2}O_{3-\alpha}$ on the oxygen partial pressure, pO_2, was studied. The oxygen partial pressures were varied by mixing O_2, air, Ar, and H_2 in the proper ratio. The typical experimental result is presented in Figure 2. It is clear that the conductivity is almost independent of pO_2, confirming that $La_{0.9}Sr_{0.1}Ga_{0.8}Mg_{0.2}O_{3-\alpha}$ is almost a pure ion conductor over the oxygen partial pressure range of 1 to 1×10^{-20} atm. This is analogous to the result reported by Ishihara.[20] From this result, it may be said that the conductivities under the various atmospheres as shown in Figure 1 are ionic. Because water vapor exists to some extent in the atmosphere and the reaction

$$2H_2O = 2H_2 + O_2$$

may occur, Figure 2 also may be expressed as a relation of log σ vs hydrogen partial pressure, pH_2, which increases from right to left in the cross axle.

We investigated the proton conduction in the specimen in the presence of water vapor or hydrogen by various electrochemical methods as described below.

Isotope Effect on the Conductivity. An isotope effect on the conductivity when using D_2O-Ar instead of H_2O-Ar as the atmosphere was observed. As shown in Figure 1, at all temperatures, the conductivity in the H_2O-Ar atmosphere is higher than that in the D_2O-Ar atmosphere, with an activation energy difference of about 0.34 kJ mol^{-1}. The increase in bulk resistance under the D_2O-Ar atmosphere may be attributed to the decrease in mobility of the charge carrier, the hydroxyl group ($OD_O^{\bullet}$). This isotope effect suggests that $La_{0.9}Sr_{0.1}Ga_{0.8}Mg_{0.2}O_{3-\alpha}$ is not only an oxide-ion conductor but also a proton conductor. Similar results have been found for $La_{0.9}Sr_{0.1}Sc_{0.9}Mg_{0.1}O_{3-\alpha}$[23] and $Sr_2(Ga_{1.1}Nb_{0.9})O_{6-\alpha}$.[24]

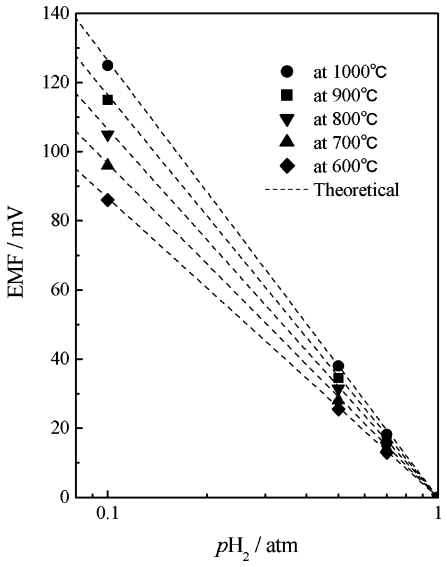

Figure 3. EMFs of the hydrogen concentration cell: H_2, Pt | $La_{0.9}Sr_{0.1}Ga_{0.8}Mg_{0.2}O_{3-\alpha}$ | Pt, H_2-Ar. Dotted line indicates the theoretical value at each temperature. Thickness of the electrolyte is 1 mm.

Electromotive Force (EMF) of Hydrogen Concentration Cell. A hydrogen concentration cell was constructed using the specimen as an electrolyte diaphragm. Pure hydrogen at 1 atm and a mixture of hydrogen and argon were applied as the electrode gases. The electrode with a higher pressure of hydrogen gas is the negative electrode. The dotted line stands for the theoretical electromotive force E_{cal} at each temperature.

According to the report by Shimura,[25] if the specimen is a proton conductor and the partial pressure of water vapor in both of the electrode chambers is the same, E_{cal} can be obtained from the following Nernst's equation

$$E_{cal} = \frac{RT}{2F} \ln \frac{pH_2(I)}{pH_2(II)}$$

where $pH_2(I)$ and $pH_2(II)$ represent, respectively, the hydrogen partial pressure in anode and cathode chamber, whereas R, T, and F have their usual meanings. If the specimen is an oxide-ion conductor and the partial pressure of water vapor in both the electrode chambers is the same, the E_{cal} can be given as

$$E_{cal} = \frac{RT}{4F} \ln \frac{pO_2(II)}{pO_2(I)} = \frac{RT}{2F} \ln \frac{pH_2(I)}{pH_2(II)}$$

where $pO_2(II)$ and $pO_2(I)$ are the oxygen partial pressures in the cathode and anode chambers, respectively. Obviously, both of the E_{cal} equations have the same form, meaning that the EMF of the hydrogen concentration cell gives the sum of the proton and oxide-ion contributions.

Figure 3 shows the EMF response of the cell to hydrogen partial pressure, pH_2. The solid symbols in Figure 3 stand for the observed EMFs. As shown in this figure, each observed value E_{obs} was close to the corresponding theoretical

(24) Liang, K. C.; Nowick, A. S. *Solid State Ionics* **1993**, *61*, 77.
(25) Shimura, T.; Esaka, K.; Matsumoto, H.; Iwahara, H. *Solid State Ionics* **2002**, *149*, 237.

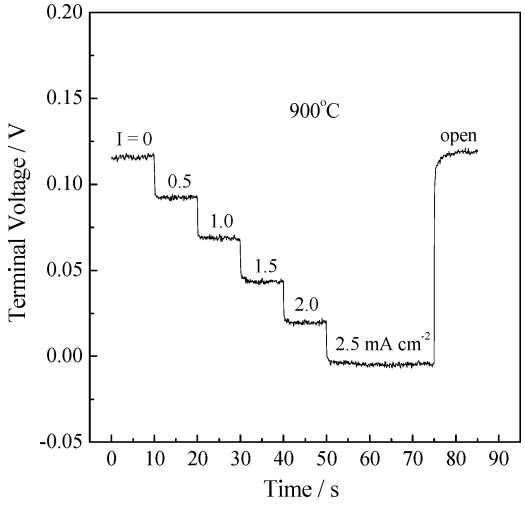

Figure 4. Discharge curve of the hydrogen concentration cell: H_2, Pt | $La_{0.9}Sr_{0.1}Ga_{0.8}Mg_{0.2}O_{3-\alpha}$ | Pt, H_2-Ar ($pH_2 = 0.1$ atm). I is the current density drawn from this cell. Thickness of the electrolyte is 1 mm.

value E_{cal} and the relationship between the E_{obs} and the logarithm of pH_2 was linear. The ionic transport number, t_i, which was determined from $E_{obs}/E_{cal} = t_i$, was almost unity at temperatures from 600 to 1000 °C in a hydrogen atmosphere, indicating that the conductivity in a hydrogen atmosphere shown in Figure 1 was purely ionic. This is in accordance with the conductivity measurements as shown in Figure 2.

We measured the discharge characteristics of the hydrogen concentration cell. As shown in Figure 4, a steady and stable current could be drawn from the cell, confirming that the charge carriers in the ceramic specimen in a hydrogen atmosphere were ions, because only hydrogen or oxygen (impurity in H_2-Ar mixture) could be supplied from the electrode chambers.

Electrochemical Hydrogen Permeation. To verify the proton conduction in the specimen directly, we performed an electrochemical hydrogen permeation (hydrogen pumping). If the specimen is a proton conductor, when a direct current is sent to the electrolytic cell, H_2 will become protons by losing electrons on the anode surface, which permeate through the specimen to the cathode, where protons obtain electrons and turn into H_2. The evolved hydrogen at the cathode was detected by a hydrogen detector, and the hydrogen evolution rate was calculated. The theoretical rate was calculated from Faraday's law. The hydrogen evolution rate as a function of current density at 900 °C is shown in Figure 5. The dependence of the hydrogen evolution rate on the current obeyed Faraday's law when the current density was lower than 10 mA cm^{-2}, indicating that the charge carriers in the specimen are protons in a hydrogen atmosphere. In other words, the conductivity of the specimen in the hydrogen atmosphere shown in Figure 1 and the ionic transport number $t_i = 1$ obtained from Figure 3 represent protonic. On the other hand, as shown in Figure 5, when the current density was higher than 10 mA cm^{-2}, the hydrogen evolution rate deviated from the theoretical value. The origin of this deviation is not clear yet. It may be relevant to the electrode polarization and a limiting proton current due to low hydrogen concentration at the interface between the electrode material (Pt) and electrolyte.[13]

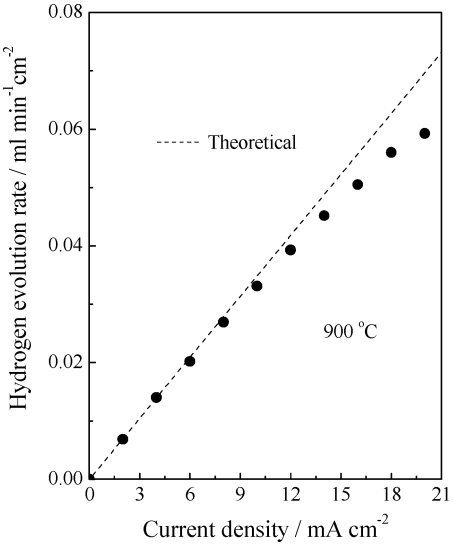

Figure 5. Hydrogen evolution rate as a function of current density at 900 °C. Dotted line shows the theoretical value calculated from Faraday's law, assuming that the specimen is a pure proton conductor. Thickness of the electrolyte is 1 mm.

Proton Conduction in Water-Vapor-Containing Air. To investigate proton conduction in water-vapor-containing air, we constructed the steam concentration cell

wet air (pH_2O(I)),

$$\text{Pt} \mid La_{0.9}Sr_{0.1}Ga_{0.8}Mg_{0.2}O_{3-\alpha} \mid \text{Pt, wet air } (pH_2O(II))$$

in which $pH_2O(I) > pH_2O(II)$ and $pH_2O(I)$ and $pH_2O(II)$ were controlled by letting air pass through water at 40 and 0 °C, respectively. The electrode with higher humidity is the negative pole (anode), whereas the electrode with lower humidity is the positive pole (cathode). If the specimen has proton conduction, the following electrode reactions can occur

$$\text{cathode: } 2H^+ + \frac{1}{2}O_2 + 2e^- \rightarrow H_2O$$

$$\text{anode: } H_2O \rightarrow 2H^+ + \frac{1}{2}O_2 + 2e^-$$

The theoretical EMF, E_{cal}, of this cell can be calculated from the following Nernst's equation, assuming the specimen is a pure proton conductor.

$$E_{cal} = \frac{RT}{2F}\ln\left(\frac{pH_2O(I)}{pH_2O(II)}\right)\left(\frac{pO_2(II)}{pO_2(I)}\right)^{(1/2)}$$

Because $pO_2(I)$ and $pO_2(II)$ are almost equal under high-oxygen partial pressure conditions, the E_{cal} may be given as

$$E_{cal} = \frac{RT}{2F}\ln\left(\frac{pH_2O(I)}{pH_2O(II)}\right)$$

When the specimen has some oxide-ion or electronic conduction, the measured EMF, E_{obs}, is lower than E_{cal}. The proton transport number, t_{H^+}, can be determined by

$$t_{H^+} = E_{obs}/E_{cal}$$

Figure 6 shows the EMF results of the water vapor

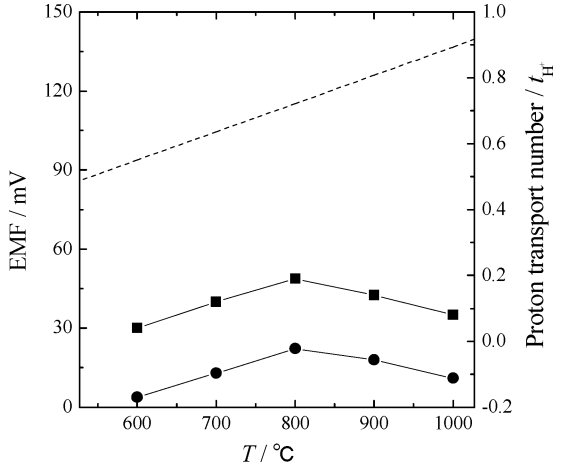

Figure 6. EMF (●) of the steam concentration cell: wet air (pH_2O(I) = 0.073 atm), Pt | $La_{0.9}Sr_{0.1}Ga_{0.8}Mg_{0.2}O_{3-\alpha}$ | Pt, wet air (pH_2O(II) = 0.006 atm), and proton transport number (■) of the specimen in wet air. Dotted line indicates the theoretical value at each temperature. Thickness of the electrolyte is 1 mm.

concentration cell. A very stable EMF is observed, indicating that the specimen has proton conduction with a t_{H^+} of 0.05−0.20 in a water-vapor-containing air atmosphere in the temperature range of 600−1000 °C, although the measured proton transport number is much lower than unity. The reason for the lower proton transport number is due to the existence of oxide-ion conduction in the specimen in water-vapor-containing air. This can be interpreted from the dependence of conductivity of $La_{0.9}Sr_{0.1}Ga_{0.8}Mg_{0.2}O_{3-\alpha}$ on oxygen partial pressure as shown in Figure 2. As mentioned above, the specimen is almost a pure ion conductor with an almost constant conductivity over the range of oxygen partial pressures, including air atmosphere. Obviously, the specimen is a mixed-ion (proton + oxide ion) conductor, and the proton and oxide-ion transport numbers are about 0.05−0.20 and 0.95−0.80, respectively, under the water-vapor-containing air atmosphere. Besides, as shown in Figure 6, the proton transport number, t_{H^+}, increases from 0.05 to 0.20 as the operating temperature is increased from 600 to 800 °C. This may be attributed to the acceleration of the following defect reactions and increase in the proton concentration, [$OH^\bullet$], under high-oxygen partial pressure conditions.

$$H_2O\,(g) + 2O_o^x + 2h^\bullet \rightarrow 2OH_o^\bullet + \frac{1}{2}O_2$$

$$H_2O\,(g) + O_o^x + V_o^{\bullet\bullet} \rightarrow 2OH_o^\bullet$$

When above 800 ˚C, t_{H^+} decreases with operating temperature, attributed to the rapid loss of H_2O from the specimen. The variation in EMF and t_{H^+} is analogous to the observation for $SrZr_{1-x}Yb_xO_{3-\alpha}$.[26]

The proton conduction in water-vapor-containing air suggests that the total ion conductivities shown in Figure 2 are mixed ionic (protonic + oxide ionic). However, the conductivities and transport numbers of proton or oxide ion in Figure 2 may vary with pO_2 or pH_2 in the atmosphere. That is, the conductivity and transport number of the proton increase and the conductivity and transport number of the

(26) Yajima, T.; Suzuki, H.; Iwahara, H. *Solid State Ionics* **1992**, *51*, 101.

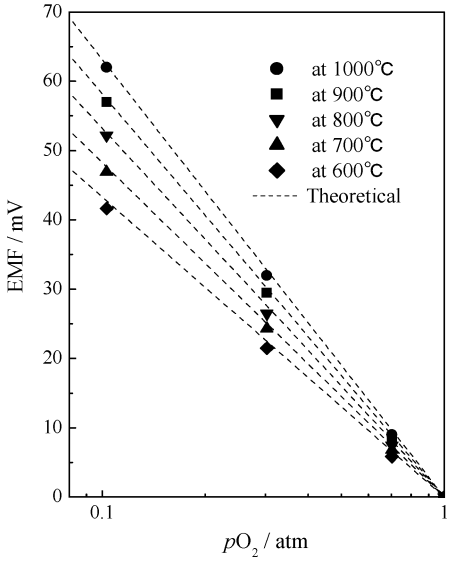

Figure 7. EMF of the oxygen concentration cell: dry O_2−Ar, Pt | $La_{0.9}Sr_{0.1}Ga_{0.8}Mg_{0.2}O_{3-\alpha}$ | Pt, dry O_2. Dotted lines indicate the theoretical values at each temperature. Thickness of the electrolyte is 1 mm.

oxide-ion decrease as pO_2 is decreased or pH_2 is increased in the atmosphere. The variations may relate to the following reactions

$$H_2 + 2O_o^x \rightarrow 2OH_o^\bullet + 2e'$$

$$\frac{1}{2}O_2 + V_o^{\bullet\bullet} \rightarrow O_o^x + 2h^\bullet$$

The increase in pH_2 may lead to the increase in proton concentration (in the form of $OH_o^\bullet$) and protonic conductivity of the specimen. On the other hand, the decrease in pO_2 with increasing hydrogen partial pressure may lead to the decrease in the reaction rate between O_2 and $V_o^{\bullet\bullet}$ and oxide-ionic conductivity of the specimen. This is why the specimen showed a significantly higher protonic transport number in reducing conditions than in oxidizing conditions, as shown in Figures 3 and 6. This is analogous to the observation for $CaZr_{0.95}Rh_{0.05}O_{3-\alpha}$ by Shimura.[25] However, there is a difference in the curves of oxygen pressure dependence of the conductivity for the two oxides. For $CaZr_{0.95}Rh_{0.05}O_{3-\alpha}$, with decreasing oxygen partial pressure, a gradual increase in the total ion conductivity is observed,[25] whereas for $La_{0.9}Sr_{0.1}Ga_{0.8}Mg_{0.2}O_{3-\alpha}$, the extent of the increase in protonic conductivity and decrease in oxide-ionic conductivity seem to be equal, but the total ionic conductivity and total ionic transport number almost do not change, as shown in Figure 2.

It may be expected that $La_{0.9}Sr_{0.1}Ga_{0.8}Mg_{0.2}O_{3-\alpha}$ would show obviously mixed-ion (proton + oxide ion) conduction and, moreover, that the proton transport number would decrease and the oxide-ion transport number would increase with increasing temperature under H_2/air fuel cell conductions. This may be analogous to the case of $BaCe_{1-x}Sm_xO_{3-\alpha}$ and $BaCe_{0.9}Yb_{0.1}O_{3-\alpha}$ under fuel cell conditions.[27,28] Detailed studies are in progress.

(27) Iwahara, H.; Yajima, T.; Ushida, H. *Solid State Ionics* **1994**, *70/71*, 267.
(28) Iwahara, H.; Yajima, T.; Hibino, T.; Ushida, H. *Solid State Ionics* **1993**, *140*, 1687.

It is well-known that some $BaCeO_3$-based perovskite oxides and complex perovskite $Ba_3Ca_{1.18}Nb_{1.82}O_{9-\delta}$ are superior proton conductors because of their higher proton conductivity and proton transport number in a hydrogen-containing atmosphere. Besides, they also show oxide-ion conduction in an oxygen-containing atmosphere.[17,19,29] The present results clearly exhibited that $La_{0.9}Sr_{0.1}Ga_{0.8}Mg_{0.2}O_{3-\alpha}$ is a superior proton conductor in a hydrogen atmosphere and a mixed proton and oxide-ion conductor in water-vapor-containing air atmosphere compared to $BaCeO_3$-based oxides and $Ba_3Ca_{1.18}Nb_{1.82}O_{9-\alpha}$.

Oxide-Ion Conduction in Dry Oxygen-Containing Atmosphere. To investigate the oxide-ion conduction in the specimen in a dry oxygen-containing atmosphere, we measured the EMF of the oxygen concentration cell using the specimen as solid electrolyte. Dry oxygen at 1 atm and a dry mixture of oxygen and argon were supplied to the cathode and anode chamber, respectively. The results are shown in Figure 7. It is clear that the measured EMF values coincide with the theoretical ones, indicating that this specimen is a pure oxide-ion conductor in a dry oxygen-containing atmosphere.

(29) Du, Y.; Nowick, A. S. *Solid State Ionics* **1996**, *91*, 85.

Conclusions

In this study, $La_{0.9}Sr_{0.1}Ga_{0.8}Mg_{0.2}O_{3-\alpha}$ was discovered for the first time to be a superior proton conductor with proton conductivity of 1.4×10^{-2} to 1.4×10^{-1} S cm^{-1} and proton transport number >0.99 in a hydrogen atmosphere at temperatures from 600 to 1000 °C. The conductivity in a H_2O-Ar atmosphere was higher than that in a D_2O-Ar atmosphere. This isotope effect on the conductivity offered a demonstration of the proton conduction in the specimen. The rate of the electrochemical hydrogen permeation (hydrogen pumping) through the specimen coincided with the theoretical rate calculated from Faraday's law. This result directly demonstrated the proton conduction in the specimen. In the water-vapor-containing air, the specimen was a mixed-ion (proton + oxide ion) conductor. The total ion conductivity was almost independent of oxygen partial pressure in the range of 1 to 1×10^{-20} atm. In dry-oxygen-containing atmospheres, the specimen was a pure oxide-ion conductor.

Acknowledgment. This study was supported by the Natural Science Foundation of China (20171034).

CM0612954